Towards Acoustic Modelling of an Oscillating Water Column in OpenFOAM

by

Yousef Beiruty

Submitted to the
Department of Fluid Mechanics of the
Budapest University of Technology and Economics
in partial fulfillment of the requirements for the degree of

Master of Science in Mechanical Engineering Modelling

December 2020

Certified by.....

Josh Davidson
Research Fellow
Thesis Supervisor

Department of Fluid Mechanics
Faculty of Mechanical Engineering
Budapest University of Technology and Economics

Towards Acoustic Modelling of an Oscillating Water Column in OpenFOAM

by

Yousef Beiruty

Submitted to the Department of Fluid Mechanics
on December, 2020, in partial fulfillment of the
requirements for the degree of
Master of Science in Mechanical Engineering Modelling

Abstract

The popularity of electrical power generation from renewable energy resources has been increasing a lot in the last decades. Ocean energy in addition to other traditional renewable resources has been sparking a greater interest in researchers. This is because it appeared as an important and promising renewable energy resource due to its enormous reserves and wide distribution. It might be a practical long-term solution for satisfying the electricity demand for countries with coasts facing the ocean. Ocean energy includes many types, the most important one is wave energy. The potential of this source of energy is great, and exploiting it efficiently can be a great step towards meeting renewable energy targets.

Oscillating water columns (OWC), are a type of wave energy converters which operate by converting wave energy into pneumatic energy, whereby wave oscillations change water levels inside of a chamber to force entrapped air through a turbine. One potential drawback of this concept is the noise generated by the turbine. In order to investigate and reduce the noise created by OWC turbines, an acoustic model of the turbine operation must be developed. However, to replicate the turbine operation in the acoustic model, it is first necessary to model the rest of the OWC system to provide information on the operating conditions. This project will involve the development of turbine model, using the Open-Source CFD software OpenFOAM, which is to be coupled to a Numerical Wave Tank (NWT).

Thesis Supervisor: Josh Davidson
Title: Research Fellow

Contents

List of Figures

List of Tables

Chapter 1

Introduction

1.1 Introduction

In the last decades, renewable energy has become increasingly popular for electricity generation, reaching excellent prospects in the market. In addition to traditional renewable energy resources such as solar, wind, and geothermal energy, ocean energy has been attracting attention. It appeared as an important and promising renewable energy resource due to its vast reserves and wide distribution. It can be a valuable solution to satisfy the electricity demand for countries with coasts facing the ocean if it was exploited extensively [6, 8, 9].

This type of energy source includes ocean tidal energy, wave energy, energy from marine currents, thermal gradient energy, and salinity gradient energy [3, 10]. The potential of wave energy is greatest amongst these and exploiting those resources would be a big step towards meeting renewable energy targets. Wave energy harvesting technologies are considered immature and in their pre-commercial phase relative to traditional renewable energy technologies such as solar, wind and geothermal. It is currently the subject of intensive research and development to reach the goal of industrial exploitation. Developing those technologies as the renewable energy market is growing will aid in achieving significant economic, environmental, and social objectives in the coming decades [11, 12].

A series of technologies, known as wave energy converters (WECs), have been

developed to extract energy from waves and convert it to mechanical energy or electrical energy [13–15]. The development of these technologies needs to address specific features like the amplitude, energy, and direction of sea waves which vary randomly through the year. Moreover, wave shapes can be massively affected by the characteristics of the coastline. Even though real condition trials are essential in evaluating the feasibility of WECs and their endurance in hostile environments, such as the sea, neither computer simulation nor laboratory testing can effectively assess the WECs' performance in any weather so far. Because of that, research in this area is still a challenge although many studies have been carried out [11, 16].

Currently, the majority of prototypes and projects for WECs are designed to operate offshore (50-70m depth). Nevertheless, among all WECs, the Oscillating Water Column (OWC) is one of the few devices that have reached the full scale prototype development stage, the one which has been studied to a greater extent and the most widely employed device to capture wave energy [3, 17]. A wide range of research on OWCs has been ongoing since the 1970s to estimate the energy yield at a given location and to optimize the efficiency with the use of parametric studies [18]. The reasons behind this intensive interest in OWCS are the simplicity of structure, operation and maintenance of OWCs as compared to other WECs [8]. Another factor is their ability of operating for long periods with high reliability and survivability. OWCs can be used to build power plants of various sizes and power ratings, with a low environmental impact and an acceptable performance which can be further improved in the future [11].

A schematic view of the OWC device with a Well turbine is shown in Figure 1-1. The OWC technology harnesses the energy from waves by using a rising and falling water surface in an air compression chamber to create a bidirectional air flow. This flow is then used to drive a turbine rotating at a high velocity connected to a conventional electric generator [9]. The simplicity of the system is coming from the energy conversion mechanism, as the only moving part is the rotor of the turbine, which is located above the water level. In order to avoid a complex and expensive system the turbine should rotate unidirectionally regardless of the air flow direction [19]. Partic-

ularly, for an OWC plant, it is important to capture the pneumatic energy from the reciprocating airflow efficiently. In the past, OWCs were equipped with non-return valves and a traditional air turbine, such as the Francis turbine or other axial-flow turbines. Unfortunately, the complicated mechanical structure of this rectifying system made it impractical for large-scale plants due to the difficulties in manufacturing and maintenance, and this was demonstrated in the sea-trial of a two-valve traditional turbine [8].

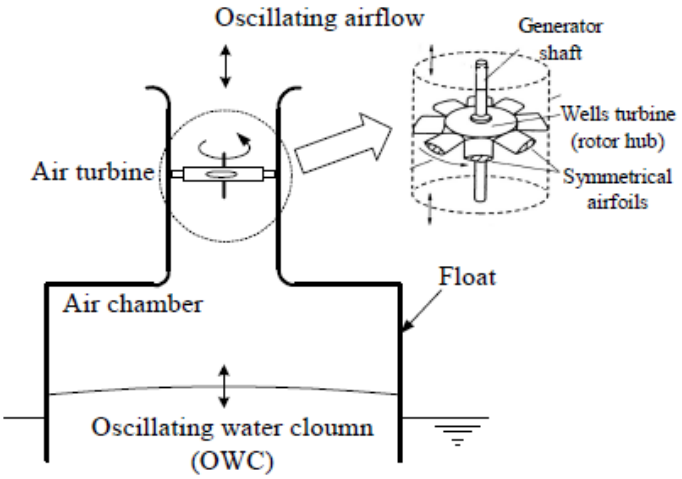

Figure 1-1: Schematic Diagram of a Typical OWC Device with the Wells Turbine [1].

As a result, the concept of a self-rectifying air turbine was proposed as an alternative due to its ability to rectify the airflow by the turbine itself directly. These turbines are able to keep the same rotation direction despite the incident airflow direction [20]. The most popular self-rectifying air turbines include the impulse turbine and the Wells turbine. The impulse turbine has been undergoing rapid development as it has several advantages over the Wells turbine in terms of a wider operating flow range, better self-starting performance, and lower working noise. On the other hand, the Wells turbine is one of the most common and most suitable for energy conversion from oscillating air flow, because of its simple geometry, high operating efficiency, low expense on fabrication and maintenance, and it is more suitable for a higher rotational regime [6]. Nonetheless, it has some drawbacks when compared to

conventional turbines, as a sudden significant decrease in efficiency can be observed over the stalling point, in addition to other disadvantages, such as poor self-starting capability, high operating noise, and low efficiency for large coefficients [8, 20].

1.2 Objectives

The goal of this thesis is to model and investigate a Wells Turbine in Open Field Operation and Manipulation (OpenFOAM) Open-Source CFD software toolbox and have it coupled to a Numerical Wave Tank (NWT). This will be a step towards achieving an acoustic model of an Oscillating Water Column, where noise will be investigated to be attenuated and reduced. Detailed explanation will be given in the Thesis Structure section.

OWCs have a low environmental impact, but their main drawback is the high operating noise to the surroundings. The end goal of this project is to reduce this noise so that more OWC projects can be implemented on-shore and near-shore to be able to harness more of the available marine energy and its great potential. This thesis will be a step in the process of a 5-year project, as many people will be working together and collaborating for the end goal.

1.3 Thesis Structure

After the current Chapter 1 which introduces the motivation of the work, objectives and structure, Chapter 2 discusses the state of art, it starts with the definition of the wave energy, its advantages and challenges. As well as, a general overview on the WEC is introduced. After that, the chapter does a theoretical study on the OWC and their operation principle and the main parts of the system. The third part of this chapter talks about the air turbines and focusing on the main two types that are popular in OWC systems. The last part of the chapter discusses the noise problem in such systems.

Later, in Chapter 3 an explanation about the case setup is done. Starting by

selecting the representative turbine and creating the geometry. Then an introduction about OpenFOAM software is presented with it advantages and disadvantages. After that the chapter discusses the steps required of seting up the case.

After that, the results of the work is presented and commented in Chapter 4. The turbine-chamber coupling and its importance are discussed in the first part of chapter 5, the second part discusses the general coupling methods which are one-way coupling and the two-way coupling, the differences, the advantages and disadvantages of each method is presented in that part as well. Finally, Chapter 6 will include the conclusion of the project and the future recommendations.

Chapter 2

State of Art

2.1 Wave Energy

Wave energy can be defined as a concentrated form of solar energy. The wind is generated by the differential heating of the earth which passes over open bodies of water, transferring some of their energy to form waves. The amount of energy transferred, and hence the size of the resulting waves, depends on the wind speed, the length of time for which the wind blows and the distance over which it blows (the fetch) [2]. These waves can be many meters in height and contain a great amount of energy. It is estimated that the potential worldwide wave power resource is 2TW [21, 22]. The highest energy waves are centered in the western coasts in the 40°–60° latitude range north and south. The power in the wave fronts varies in these areas between 30 and 70 kW/m with peaks to 100kW/m in the Atlantic SW of Ireland, the Southern Ocean and off Cape Horn. This resource is capable of providing 10% of the current level of world electricity supply, if harnessed in a convenient way [1, 21]. Approximate global distribution of wave power levels in kW/m of wave front is shown in Figure 2-1.

The physical law of conservation of energy requires that the energy-extracting device must interact with the waves such as to reduce the amount of wave energy that is otherwise present in the sea [23]. The possibility of generating electrical power from these deep water waves has been realized for many years, and there are

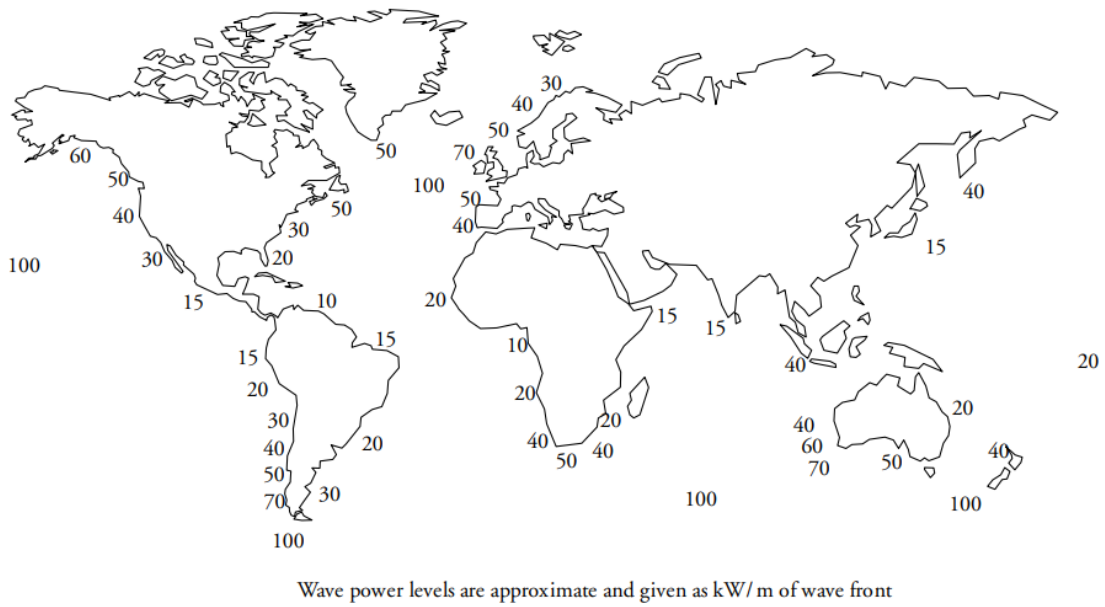

Figure 2-1: Wave power levels are approximate and given as kW/m of wave front [2]

countless ideas and technologies to extract the power. These technologies will be discussed in the next section, but before that, it is interesting to demonstrate the main advantages of extracting wave power and the challenges that stand in the face of these technologies.

2.1.1 Advantages

Ocean waves offer the highest density among other renewable energy resources, as the high density stems from the large mass density of water compared to air (1000 times greater). This results in a much higher average power production from waves per unit of time. In addition to that, the natural seasonal variability of wave energy follows the electricity demand in temperate climates, and power from ocean waves continues to be produced around the clock, unlike wind and solar powers. Furthermore, ocean waves travel great distances without significant energy losses, so they act as a renewable source beside being an efficient energy transport mechanism across thousands of kilometers [24, 25].

2.1.2 Challenges

On the other hand, there are certain difficulties and technical challenges facing wave energy that need to be overcome to enhance the performance of WECs and make them commercially competitive in the energy market.

Wave patterns are irregular and vary considerably in amplitude, phase, and direction, and thus, it is difficult to design devices to extract power efficiently over this wide range of variables. It is challenging to capture this irregular motion efficiently, as the device and its corresponding systems need to be rated for the most common wave power level to be considered efficiently operating [26].

The device should also be able to withstand extreme wave conditions such as extreme gales or hurricanes. This does not only challenge the structural design of the device, but causes economic challenges as well. The normal output of the device (and hence the revenue) are produced by the most commonly occurring waves, apart from the capital cost of the device construction which is driven by a need to withstand the high power level of the extreme, yet infrequent waves [22]. Moreover, Wave periods are commonly around 0.1 Hz, which makes it significantly challenging to couple this irregular slow motion to electrical generators, requiring about 500 times greater frequency [26].

It is necessary and important to have a detailed evaluation of the complete system, which if optimized, a robust yet efficient system is to be developed. However, there is a huge diversity in devices that are used to harness wave power to produce electricity, and one of the most important devices will be discussed in the next section.

2.1.3 General overview on Wave Energy Converter (WEC)

The idea behind power generation from a WEC is basically that the wave energy is converted into reciprocating mechanical energy by a wave energy acquisition system at first, which will then be converted into mechanical energy through a Power Take-off (PTO) system and finally converted to electrical energy via a generator set and output [13]. Some of the main obstacles facing the deployment of these devices are

the high costs of installation and maintenance for the power plants, uncertainty of results, and technological problems [11].

Nonetheless, over the years a wide variety of WECs have been developed, nowadays over 1000 wave energy conversion techniques have been patented in Japan, North America, and Europe [22]. Mainly, WECs can be categorized according to three characteristics [15, 22]:

1. Location: it is defined as a function of the distance from the coast. There are three types of converters: Onshore, Nearshore and Offshore devices.

2. Device size and directional wave characteristics: it is classified according to the size and the direction of the device regarding the incoming wave. They are classified into three types: Attenuator, Point Absorber and Terminator.

3. Modes of operation: this is a further level of classification of devices, determined by their mode of operation. Some significant examples are: Submerged pressure differential, Oscillating wave surge converter, Oscillating water column and Overtopping device.

The following section gives detailed information about the most famous mechanism to convert wave energy to mechanical energy, namely, the Oscillating Water Column (OWC) mechanism. The OWC provides the simplest and possibly the most reliable means of converting slow irregular wave motion into high speed rotational movement required for electrical power generation.

2.2 Oscillating Water Column (OWC) principle

2.2.1 Oscillating Water Column (OWC)

Among the myriad of systems mentioned before for harnessing wave energy, the concept of the OWC system is unique and different, as it is the only technology where a key part of the system can be seen as a naturally occurring structure [27]. This type of wave energy converter is considered more attractive over the other types because

of the simplicity of its structure, operation and maintenance [8]. This is due to the fact that the only moving part in the whole system is the air turbine, as there are no moving parts submerged in water, which makes it easy to maintain, and improves reliability. Thus, the OWC system has the ability of operating for long-terms with high reliability and survivability [8].

However, in the past, OWCs were used for a purpose different than energy conversion and generation. The first recorded application is the whistling buoy which is used for warning purposes to aid with navigation and it goes back to the nineteenth century [27]. Later, starting from the 1970s, an extensive research on OWCs has been performed in order to assess the energy yield at a given location and to optimize the efficiency with the use of parametric studies. The main idea is to make use and take advantage of breakwaters by setting up wave energy converters in order to produce local electrical energy in coastal regions [18].

As mentioned before, the OWC has been widely employed to capture wave energy [3]. A reason for this is its structure which is fairly simple as it consists of an internal water chamber separated from the open sea by a partly submerged wall. This chamber traps the air above the free surface of water and acts as a piston. The trapped air communicates with the exterior air via an orifice containing a unidirectional turbine. The oscillating motion of the internal free surface causes the trapped air to be pressurized and depressurized consequently compared to the external air. This alternating air flux makes the turbine rotate and generate energy since it is linked to a generator [10, 18].

In other words, an OWC consists of two parts, namely: a collector chamber with valves and ducts, which transfers wave power into the air within the chamber, and a (PTO) system, which converts the pneumatic power into a useful form of energy such as electricity. The pressure in the chamber is alternately pressurized as the water column rises and rarefied as the water column falls. Typically, the PTO is an air turbine, although it is also possible to use a water pump as an alternative [28]. Since the airflow is cyclic and alternating, this air turbine is normally chosen to be of the self-rectifying type so that no matter what the direction of airflow is, the turbine is

driven in the same direction. Some examples of such turbines include Wells turbines, impulse turbines or biradial turbines, with the Wells turbine being the most commonly used type of PTO for such hydro-pneumatic devices. In addition to this, other parts include electric generators and electronic power converters, as well as, a control valve which can be mounted in the duct between the chamber and the turbine to regulate the airflow [3, 11]. See Figure 2-2.

Like most WECs, OWCs are resonant devices. The OWC concept is more efficient when the fluid between the back wall and the barrier is excited by the incident wave and works in a piston mode. Theoretically, the maximum power absorption occurs when pressure and wave induced volume flux are in phase, thus, a key point for obtaining better efficiencies is the chamber design [11, 18].

Generally, OWCs can be installed on shore, embedded in a cliff or a harbor wall, or standing on the seabed near the shore, or in a floating structure offshore in deep waters. They have shown great reliability when it comes to shore-based operations, and this reliability can be transferred to other platforms. They are used to build power plants of various sizes and power ratings, with a low environmental impact and an acceptable performance which can be further improved in the future. The OWC is the most widely used wave energy converting technology for onshore structures [29]. On the other hand, offshore OWCs have greater power at the input, but they must endure harsh weather conditions which in turn increases maintenance costs. Moreover, the cost of grid connection in offshore systems is high [11, 27].

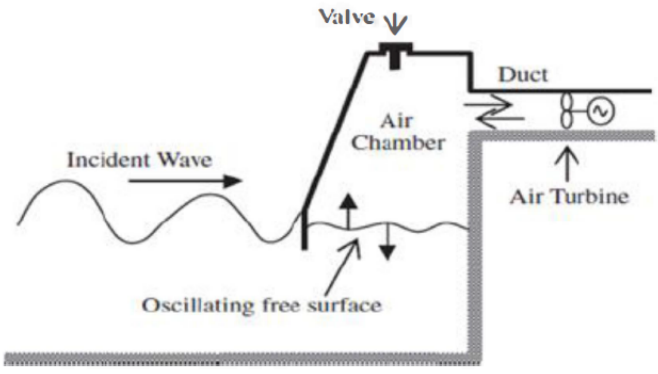

Figure 2-2: The oscillating water column system [3].

2.3 Air Turbines

Nowadays, most of the research aiming at the assessment of OWC performances focuses on Wells turbine modelling due to its approximately linear behavior characteristics pressure/flowrate. Most of onshore and nearshore OWC projects are equipped with bi-directional Wells turbines, compared to fewer projects and studies which consider impulse turbines instead [18]. These turbines will be discussed and compared in details in this section.

In an OWC, the air turbine is subject to much more challenging conditions than turbines in other applications, such as wind turbines. The flow through the turbine is reciprocating, random, and highly variable over various time scales, ranging from a few seconds to seasonal variations. It makes great sense that the time-averaged efficiency of an air turbine in an OWC is significantly lower than that of other types of turbines, including steam, gas, and wind turbines working in nearly steady conditions. [14].

Most of the early OWCs were fitted with air turbines as the PTO and are still favored till this day. Traditional axial-flow turbines such as the Francis turbine were used as the set-up for early operating OWCs, those turbines were equipped with a rectifying system and non-return valves. The reason for choosing air turbines over conventional turbines is that the latter are not suitable for reciprocating flows, and this in turn has led to the development of new types of turbines. The concept of a self-rectifying turbine, i.e. a turbine that can rotate in an unchanged direction regardless of the direction of the incident air flow, was proposed as an alternative since the use of a rectifying system proved to be unpractical. This is the reason why a great deal of published papers took interest in self-rectifying turbines than any other piece of equipment for OWCs [4, 5, 30].

It is vital to efficiently-capture the pneumatic energy from the reciprocating flow for an OWC plant. Unless check valves are used, self-rectifying air turbines are used to equip OWCs inside which the air alternately flows from the chamber to the atmosphere and back, and so the turbines need to be unidirectional for such bidirectional flow. Two main types of self-rectifying turbines in use so far are impulse

turbines and Wells turbines [8].

2.3.1 Wells Turbine

The Wells turbine was invented by Alan Arthur Wells in 1976. As mentioned previously, the reason why it grabbed attention in OWC plants was its simple geometry and its high operating efficiency [8]. The Wells Turbine is one of the simplest and probably the most economical turbines for wave energy conversion. There is no need for rectifying air valves, and the power can be extracted at low airflow rates while other turbines would be inefficient. Therefore, it has been extensively researched and developed in many countries [25].

The Wells turbine, which is an axial-flow self-rectifying turbine, rotates unidirectionally in reciprocating airflows generated by the air chamber and thus plays a major role in pneumatic power conversion [8, 14]. The turbine consists of a rotor with symmetric airfoil type blades placed around a central hub and rotates in one direction irrespective of the direction of the airflow [4, 25], as shown in Figure 2-3. The rotational speed is limited by the blade tip velocity approaching the speed of sound. The Wells turbine works on the general aerodynamics theory of airfoil. Blades are set at 90∘ stagger angle. The absolute velocity of air hits the blade axially and the tangential velocity of the blade acts in a direction parallel to the plane of rotation. The relative velocity acting at an angle, known as the angle of attack (α), to the blade causes a lift force perpendicular to the direction of relative velocity and a drag force in the direction of relative velocity. These lift and drag forces can be combined to get the tangential force [4, 26]. The direction of rotation of the turbine always remains the same, since the direction of tangential force is always the same for any airflow direction. However, the lift and drag forces on the airfoil increase up to a certain value of the angle of attack (α), which if exceeded, the flow will separate around the airfoil. The angle at which flow separates from the airfoil is known as the stall angle. Beyond the stall angle, the lift force decreases and the drag force increases significantly. As a result, the tangential force on the rotor decreases, leading to a decrease in efficiency. Thus, the angle of stall limits the operating range of Wells turbine.

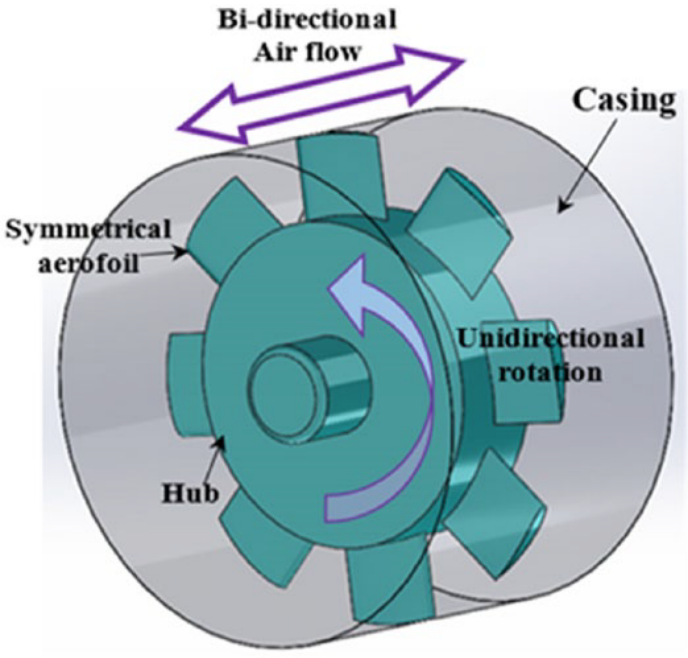

Figure 2-3: Schematic of a Wells turbine [4].

One of the best features of a wells turbine can be the high blade to air-flow velocity ratio, which means that a relatively high rotational speed may be attained for a low velocity of air flowing through the turbine, thus allowing a cheaper generator to be used while also enhancing the possibility of storing energy by the flywheel effect. Another good feature is that it has a quite good peak efficiency, which can go up to about 0.75. And finally, a Wells turbine is relatively cheap to construct. On the other hand, a Wells turbine has some disadvantages. It has a poor self-starting capability besides its high operating noise. Some other week points of the wells turbines include, a low torque at small flow rates; a drop in the power output due to aerodynamic losses at flow rates exceeding the stall-free critical value, and finally it has a relatively large diameter for its power [5, 14].

An impulse turbine, discussed in the next subsection, with fixed guide vanes and counter rotating rotors was suggested to be superior to the Wells turbine in the overall performances under irregular flow conditions. But, this turbine also suffers from the cost of balancing of the gears and from causing severe noise as well. Therefore, the main Worldwide trend for wave energy conversion systems remains to be the Wells turbine, mainly due to its extremely simple geometry [31].

2.3.2 Impulse Turbine

Impulse turbines are the most popular and the most frequently proposed alternative to Wells turbines. These turbines were patented by I. A. Babintsev in 1975 [32]. The main difference between Impulse turbines and Wells is in the way of transferring energy, that takes place in the rotor. Both turbines are defined as axial-flow self-rectifying turbines. The impulse turbine can be made to be insensitive to the airflow direction, which is due to two rows of guide vanes on both sides of the rotor instead of a single row (as in the conventional full-admission steam turbine) [4, 5, 33]. Furthermore, the guide vanes can be classified as fixed, self-pitch-controlled, and link mechanism type [4].

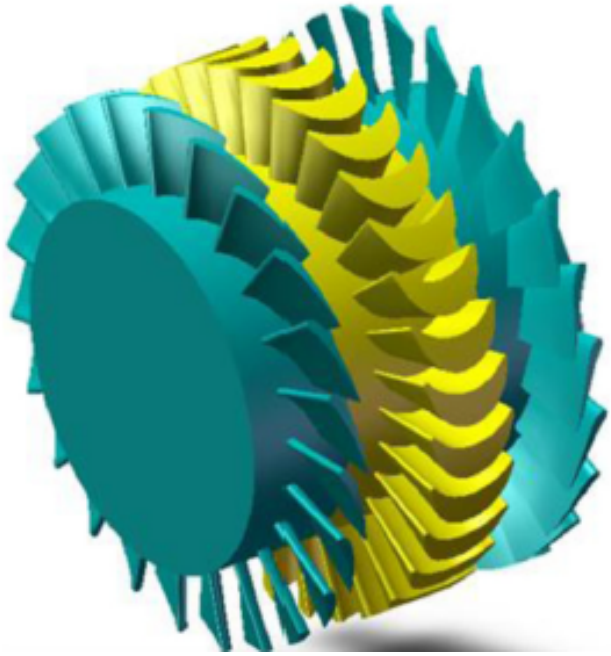

Figure 2-4: Impulse turbine [5].

The efficiency of the self-rectifying axial-flow impulse turbine with fixed guide vanes is severely affected by the losses at the entry to the downstream row of guide vanes. On the other hand, the efficiency curves do not suffer from the sharp drop typical of most Wells turbines. Compared to the Wells turbine, the impulse turbine can achieve higher efficiencies for larger flow coefficients without stall and it can also self-start in a shorter period [8]. Performance of axial-flow impulse turbines can

improve if pivoting guide vanes are used instead of fixed ones. This allows the flow from the rotor to enter the downstream row of guide vanes at a smaller angle of incidence and in turn avoid or reduce the losses due to boundary layer separation [5].

Some of the advantages of impulse turbines include a wider operational range than that of the Wells turbine and less sensitivity to flow coefficient variations. It also has a better self-starting capability due to its mechanical nature, as the Wells turbine needs approximately a six-fold longer period to start than the impulse [8, 18]. However, impulse turbines have lower rotational speeds than those of Wells turbines, about three times less, which makes impulse turbines less adapted to energy storage based on the fly-wheel effect than Wells turbines. Yet, it is expected for the future to have an effective design of the impulse turbine for OWC powerplants, especially in low-density wave climates [8].

2.4 Noise

The desire for greater implementation of full scale WECs has driven the deployment of certain technologies such as the OWC, which is one of the onshore technologies that can be deployed in the vicinity to inhabited areas, either as stand-alone projects or incorporated into breakwaters. However, due to the likely proximity of those devices to residents and to important population of marine animals such as cetaceans, both airborne and underwater noise impacts of this technology need to be assessed properly [19].

Noise can be defined as any unwanted sound that can have adverse effects on humans as well as the environment in case it interferes with natural wildlife. There is a growing awareness and concern for the potential impact of anthropogenic sources of sound that have been rising considerably over the past decades [34], mainly coming from industrial activities. This is the case for both, airborne and underwater noise.

Even though it is hard to prove the specific impact of noise categorically, the disturbance of noise on humans and wildlife has been an ongoing and an important research focus [35–37]. Thus, it is crucial to create good methodologies to assess and

monitor the noise generated by any newly introduced technology, and therefore, noise is considered an important descriptor of an Environmental Impact Assessment (EIA).

In principle, wave energy projects are expected to cause less noise than other existing maritime activities [38] such as pile driving, air gun pulses, or shipping. However, the noise emitted is highly dependent on the type of technology, number of devices, and their layout.

Unlike offshore devices, onshore technologies such as the OWC raise important noise-related issues as this device generates airborne noise that can affect humans and land fauna in proximity, in addition to underwater noise. The noise produced will be highly variable as it depends on several factors that can be hard to combine and evaluate separately. These factors include the wave climate (wave height, period and direction), morphology of the surrounding terrain, atmospheric conditions (wind direction, wind intensity, humidity) and operational conditions (wave interactions in the chamber, rotational speed, relief valve position, control law).

Chapter 3

Case Setup

3.1 Selecting a Representative Turbine

A lot of work has been done in the field of self-rectifying air turbines used in wave energy converters. Some works focused on impulse turbines, while other works focused on Wells turbines, which are the two most popular ones. In this thesis, we decided to follow this paper [6] and use the turbine and air duct geometry as a basis for our case study. A lot of adjustments were made on the geometry, as it is needed to start with the simplest case for this thesis study and then build over it step by step until we reach our end goal which will require some years. The goal is to have a simple working model of a turbine which is to be coupled with a numerical wave tank later.

3.2 Creating the Geometry

The turbine used in the paper followed, shown in Figure 3-1, is a Wells turbine with a blade profile of the NACA four-digit series with a thickness ratio of 20% and a chord length of 0.9m. 199 points representing the NACA0020 airfoil were created using a NACA 4-Digit Airfoil generator. The airfoil was created with a 0-degree angle of attack, a closed trailing edge, and the chord length was adjusted to 1m. The clearance between each tip of the airfoil and the adjacent wall is 0.17m.

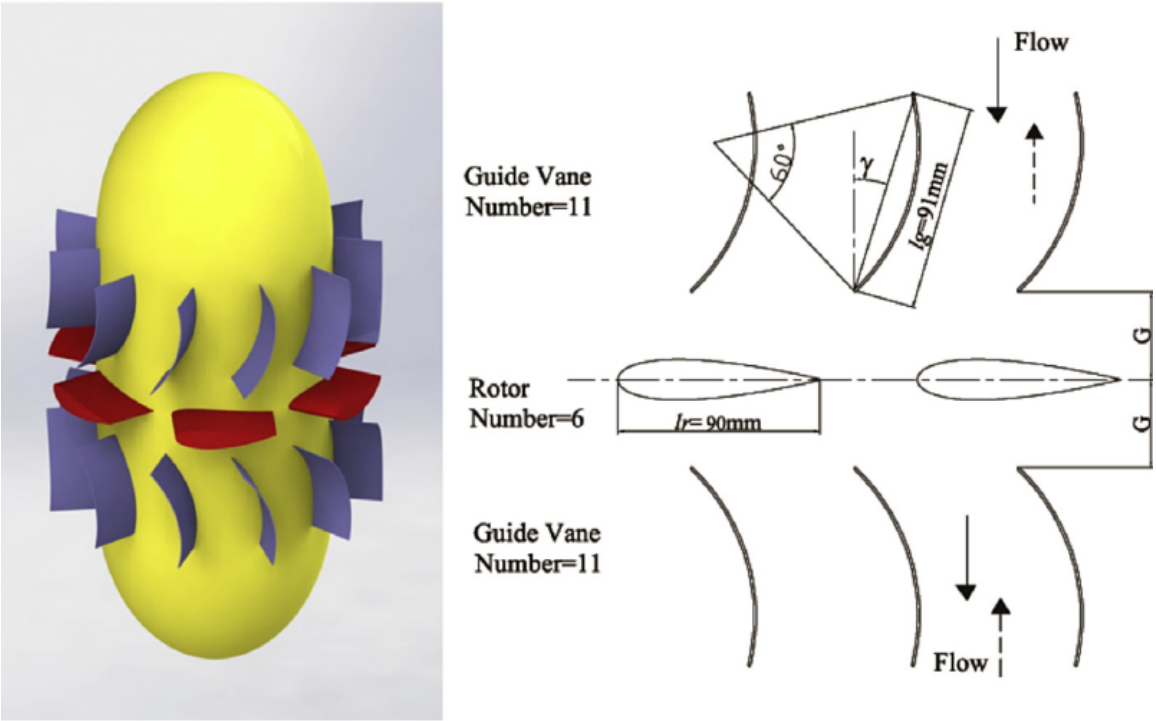

Figure 3-1: 3D sketch and turbine configuration at mean radius [6].

The airfoil was then imported into the open-source pre-processing software GMSH, which is a 3D finite element mesh generator with a built-in CAD engine and post-processor. It provides a user-friendly meshing tool with parametric input and advanced visualization capabilities. 2 out of the 4 modules of GMSH were used in this thesis work, namely Geometry, and Mesh modules. The input to these 2 modules was specified by using both the graphical user interface, and in ASCII text files using GMSH's own scripting language (.geo files).

The geometry was completed by plotting the domain in which the air will flow and interact with the turbine, which gave way for creating the mesh. Firstly, a spline connecting the points was created, followed by 4 points representing the outer geometry or the domain. Lines were drawn, followed by line loops and plane surfaces. The 2-dimensional surface was extruded by 1 cell into the z-direction, which leaves us with a 1 cell thick 3-dimensional geometry. This will be considered a 2-dimensional geometry by OpenFOAM. 7 different regions or physical surfaces were defined, namely Inlet,

Outlet, Bottom, Top, Front, Back, and Airfoil, as shown in Figure 3-2. Finally, the physical volume was defined which allows us to create the mesh. Table 3.1 describes the physical surface type for each surface label shown in Figure 3-2.

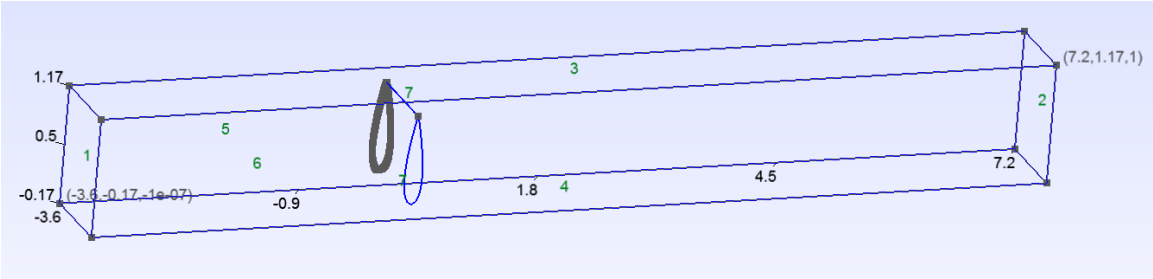

Figure 3-2: Cad model - Boundary Conditions.

Table 3.1: Names of Patches

Surface Label	**Physical Surface Type**
1	Inlet
2	Outlet
3	Top
4	Bottom
5	Back
6	Front
7	Airfoil

The mesh in Figure 3-3 shows a higher density around the airfoil, and at both the inlet and the outlet. This allows the capturing of more data in this area of interest. In order to ensure the sufficient development of flow, the computational domain was extended four and eight blade chord lengths (keeping in mind that the blade chord length was supposed to be equal to 0.9m instead of 1m) upstream and downstream of the blade, respectively.

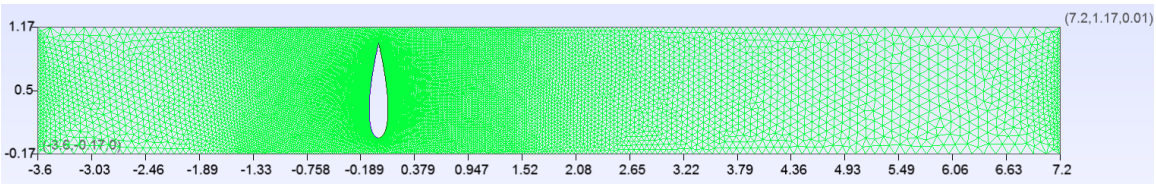

Figure 3-3: Volume Mesh.

3.3 Numerical implementation

3.3.1 OpenFOAM

Open source Field Operation and Manipulation program (OpenFOAM) is the leading free, open source software, owned by the OpenFOAM Foundation and distributed exclusively under the General Public Licence (GPL). The GPL gives users the freedom to modify and redistribute the software and a guarantee of continued free use. OpenFOAM is a C++ programming language software for the development of customized numerical solvers, and pre-/post-processing utilities for the solution of continuum mechanics problems, including computational fluid dynamics (CFD) [7, 39]. OpenFOAM utilities subdivided into [40]:

- **Geometry and Meshing:** Utilities to generate geometry like blockMesh and meshing using snappyHexMesh, foamyHexMesh etc. Can import mesh from other meshing Software like Ansys, GMsh, Salome etc.
- **Parallel Processing:** Tools to decompose, reconstruct and redistribute the computational case to perform parallel calculations, at times better than other CFD Software.
- **Post Processing Utilities:** Post processing can be done using ParaView which comes with OpenFOAM. Can export to other third party visualisation Software.

In addition to the no license cost, which means it is free for anyone to download and use, being based on the C++ language and open source, gives the ability to the user to modify, create his own solver and it can be customized to suit any workflow. Moreover, OpenFOAm has many other advantages over other CFD software, that it allows also the possibility to use all available processors for a single simulation, whereas for commercial software licences using additional processors requires additional licenses limiting the available processors to the number purchased in the license [40].

On the other hand , OpenFOAM is not controlled through a graphical user interface (GUI) unlike most of the commercial CFD softwares. Settings are adjusted

through a text files called dictionaries and everything is controlled via the command line. The absence of a GUI and of a maintained documentation makes it hard for the new users, however once got used to it, it becomes a very flexible and automated tool.

File structure of OpenFOAM cases

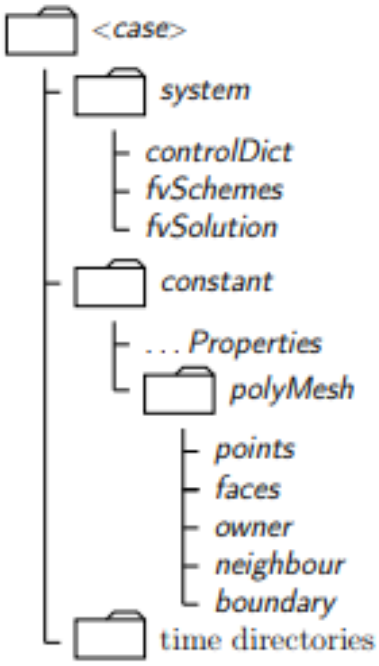

Figure 3-4: Case directory structure [7]

The basic directory structure for a OpenFOAM case, that contains the minimum set of file required to run an application, is shown in Figure 3-4, and described as follows:

1. A system directory: contains the geometry and mesh definition, numerical scheme settings and the simulation controls.

2. A constant directory: contains a full description of the case mesh in a subdirectory and the physical properties of the case.

3. The 'time' directories: contains individual files of data for particular fields, e.g. velocity and pressure. The data can be: either, initial values and boundary

conditions that the user must specify to define the problem; or, results written to file by OpenFOAM.

3.3.2 Building the Case

After being generated by GMSH, the mesh was imported to OpenFOAM. A new case folder was created and then gmshToFoam command was run for OpenFOAM to be able to read the mesh file. The command checkMesh was run afterwards to check if the mesh is acceptable for running the simulations. More details about the mesh check can be seen in the Figure 3-5.

The mesh has approximately 30,000 prism-type cells. All the mesh checks such as: max cell openness, face area magnitudes, cell volumes, non-orthogonality, and max skewness were accepted by OpenFOAM. Max aspect ratio is equal to 3.5 and average mesh non-orthogonality is equal to 4, which are also within the acceptable range.

3.3.3 Case Dictionaries

The case dictionaries is divided to three folder Constant Folder, System Folder and 0 folder.

Constant Folder

The boundary conditions were set for the 7 boundary patches. The Front and the Back patches were defined as “empty”. The Inlet and the Outlet patches were defined as “patch”. The Airfoil patch was defined as wall. The Top and the Bottom patches were defined as “wall”, even though the correct definition should have been “cyclic”, but it was decided to go with “wall” to avoid complications at this elementary stage. “Cyclic” or a rotationally periodic boundary should be employed at both, the Top and the Bottom patches, to create a numerical model with a single blade without the need of modelling all the rotors which will be computationally expensive. This way, the advantage of a smaller grid size and less computing time can be gained.

No turbulence model was used at this stage, which means that laminar simulations

```
// * * * * * * * * * * * * * * * * * * * * * * * * * * * * * * * * * * * * //
Create time

Create polyMesh for time = 0

Time = 0

Mesh stats
    points:           30408
    internal points:  0
    faces:            104112
    internal faces:   44068
    cells:            29636
    faces per cell:   5
    boundary patches: 7
    point zones:      0
    face zones:       0
    cell zones:       1

Overall number of cells of each type:
    hexahedra:     0
    prisms:        29636
    wedges:        0
    pyramids:      0
    tet wedges:    0
    tetrahedra:    0
    polyhedra:     0

Checking topology...
    Boundary definition OK.
    Cell to face addressing OK.
    Point usage OK.
    Upper triangular ordering OK.
    Face vertices OK.
    Number of regions: 1 (OK).
```

```
Checking patch topology for multiply connected surfaces...
    Patch              Faces    Points   Surface topology
    Back               29636    15204    ok (non-closed singly connected)
    Front              29636    15204    ok (non-closed singly connected)
    Top                226      454      ok (non-closed singly connected)
    Inlet              41       84       ok (non-closed singly connected)
    Bottom             226      454      ok (non-closed singly connected)
    Outlet             41       84       ok (non-closed singly connected)
    Airfoil            238      476      ok (non-closed singly connected)

Checking geometry...
    Overall domain bounding box (-3.6 -0.17 0) (7.2 1.17 0.01)
    Mesh has 2 geometric (non-empty/wedge) directions (1 1 0)
    Mesh has 2 solution (non-empty) directions (1 1 0)
    All edges aligned with or perpendicular to non-empty directions.
    Boundary openness (-8.38386e-20 -2.6929e-18 4.19736e-16) OK.
    Max cell openness = 2.91348e-16 OK.
    Max aspect ratio = 3.50743 OK.
    Minimum face area = 2.01657e-05. Maximum face area = 0.00853152.  Face area magnitudes OK.
    Min volume = 2.01657e-07. Max volume = 8.53152e-05.  Total volume = 0.143358.  Cell volumes OK.
    Mesh non-orthogonality Max: 41.9611 average: 4.02617
    Non-orthogonality check OK.
    Face pyramids OK.
    Max skewness = 0.66028 OK.
    Coupled point location match (average 0) OK.

Mesh OK.

End
```

Figure 3-5: Mesh Check

were carried out. This was defined in the "tubulenceProperties"dictionary in the "constant" folder. In the "transportProperties"dictionary, a Newtonian transport model was defined, the density was set to be equal to 1 and the kinematic viscosity equal to 10^{-5}.

System Folder

Starting with the "solvers" subsection of the "fvSolution", a GAMG (Generalised Geometric-Algebraic Multi-Grid) solver was defined for the pressure and "smooth-

Solver" with a "GaussSeidel" smoother for the velocity. A relaxation factor of 0.7 was defined in the "relaxationFactor for the velocity.

SimpleFoam was used as the solver at this stage, as a pressure-based solver is needed. SimpleFoam is a steady state solver for incompressible, turbulent low, using the SIMPLE (Semi-Implicit Method for Pressure Linked Equations) algorithm for solving both the continuity and momentum equations. This solver can be used for both laminar and RANS (e.g., k-epsilon, SST etc.) turbulence models

It was decided to use the SIMPLEC (Semi-Implicit Method for Pressure Linked Equations Consistent) algorithm instead of the SIMPLE for the pressure-velocity coupling in this thesis work. The reason for this is that SIMPLEC has a faster speed of convergence than the SIMPLE scheme. In the SIMPLEC algorithm, the momentum equations are manipulated in a way which allows the velocity correction equations to omit terms that are less significant than those omitted in SIMPLE.

It is also important to note the SIMPLEC formulation for the pressure-velocity coupling does not need using any relaxation on pressure, and a small amount of under-relaxation for velocity and other transport equations. Lastly, 2 non-orthogonal correctors were used to account for the mesh non-orthogonality.

In the first subsection of "fvSchemes", a steady-state time scheme was defined. In the second subsection, a Gauss linear discretization scheme was used as the default scheme for the gradient terms. The "Gauss" entry requires the interpolation of values from cell centers to face centers, while the "linear" entry refers to the interpolation scheme which, in this case, means linear interpolation or central differencing. The velocity gradient was overridden to improve boundedness and stability. This was done by using the "cellLimited"scheme which limits the gradient so that the face values do not fall outside the bounds of value in surrounding cells, when the cell values are extrapolated to the faces using the calculated gradient. A limiting coefficient of 1, which guarantees boundedness was specified.

All the schemes in the divergence schemes subsection are based on Gauss integration, using the flux "phi" and the advected field being interpolated to the cell faces by one of a selection of schemes. For the advection of velocity, Gauss GammaV scheme

was used with a limiter of 1. This "Gamma" entry is a blend of central differencing (CD) and upwind differencing (UD) schemes and is based on Leonard's NVD concept. The 'V' refers to a specialized version of schemes designed for vector fields. It calculates a single limiter based on the direction of the most rapidly changing gradient and is applied to all components of the vectors instead of calculating separate limiters for each vector component.

Furthermore, a corrected surface normal gradient scheme was used. The corrected scheme is an explicit non-orthogonal correction that maintains second-order accuracy and is generally recommended for meshes with max non-orthogonality less than 70. The maximum non-orthogonality in our mesh is 41.96, as can be seen in Figure 3-5. Regarding the Laplacian scheme, the Gauss scheme was selected as it is the only choice of discretization, a linear interpolation scheme was used for interpolation of the diffusivity, and a corrected scheme was used for the surface normal gradient scheme. Lastly, linear interpolation was selected in the interpolation schemes subsection.

0 Folder

- **Pressure**

Table 3.2: Pressure Boundary Fields

Boundary Field	**Type**
Inlet	freestreamPressure
Outlet	freestreamPressure
Top	zeroGradient
Bottom	zeroGradient
Back	empty
Front	empty
Airfoil	zeroGradient

As shown in table 3.2, a "freestreamPressure" boundary condition was defined for both the Inlet and Outlet. This is a 'mixed' boundary condition in which the operation mode switches between a fixed value and zero gradient based on the flux sign. A "zeroGradient" boundary condition was defined for both the Top, the Bottom,

and the Airfoil patches. This applies a zero-gradient condition from the internal fields of the patch onto the faces of the patch. Lastly, an "empty" boundary condition was defined for the Back and the Front patches.

- **Velocity**

For the velocity, it is required to use a range of input air flow conditions in the assignment sheet of this thesis namely, constant, sinusoidal oscillations, and measured oscillations from numerical wave tank experiments, respectively. More details about each flow condition will be shown in the results section

Chapter 4

Results

In this chapter, the results of the simulations for different input air flow conditions are presented. The first case is a constant velocity of 10m/s applied at the inlet. The second case is a sinusoidal oscillation, and the third case is for oscillations taken from numerical wave tank experiments. For each case, the following parameters were measured and monitored: Y+, Courant number, velocity field and pressure field averages, minimum and maximum velocity, and pressure values over the entire field, streamlines, vorticity contours, lift and drag. Furthermore, probes for measuring velocity and pressure were defined at 8 different locations around the airfoil .

4.1 Case 1

For the first simulation case, a constant input air flow condition was applied. Mainly, this was applied inside the 'U' dictionary in the '0' folder. A constant axial velocity of 10m/s was applied at the inlet. A slip boundary condition was defined at the Top and Bottom patches because the mesh was not fine enough to apply the needed no-slip boundary condition, which was tried at first, but was abandoned due to very high gradients which were accumulating next to those two walls. A noSlip boundary condition was applied at the Airfoil, and empty boundary condition for the Front and Back. A "freestreamVelocity" boundary condition, which is a mixed boundary condition between fixed value and zero gradient was applied at the

Inlet. Finally, an "inletOutlet" boundary condition was defined at the Outlet, which provides a generic outflow condition, with specified inflow for the case of return flow.

Table 4.1: Velocity Boundary Fields for Case 1

Boundary Field	**Type**
Inlet	freestreamVelocity
Outlet	inletOutlet
Top	slip
Bottom	slip
Back	empty
Front	empty
Airfoil	noSlip

4.1.1 Case 1 simulation results

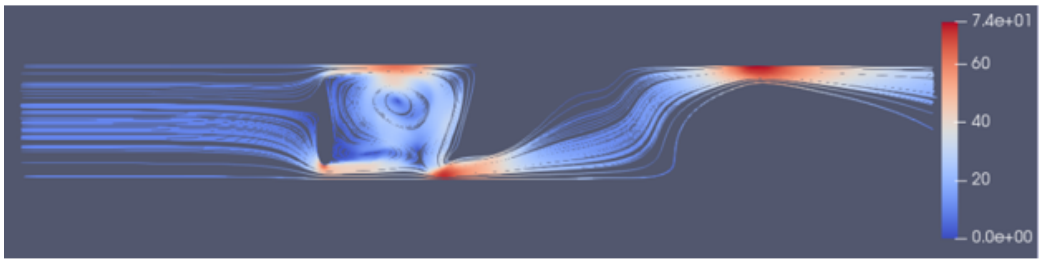

Figure 4-1: Streamlines at time = 50s

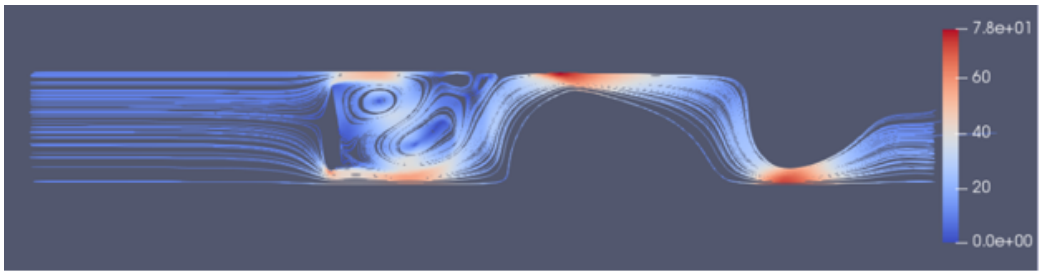

Figure 4-2: Streamlines at time = 51s

It can be seen from Figure 4-1 that the flow is behaving as a potential flow as it approaches the airfoil from the upstream region, which is characterized by an irrotational velocity field. In the downstream region, there is a huge separation zone.

A backflow is expected in the empty regions of the domain. 2 vortices can be clearly seen in Figure 4-2. The bottom vortex, which is the stronger one, generates rotation in the counterclockwise direction, while the upper vortex generates rotation in the clockwise direction. Therefore, they do not cancel each other and survive. It can be seen clearly that the flow is attached at the top and bottom walls. Secondary flows cannot be seen here due to the velocity limits.

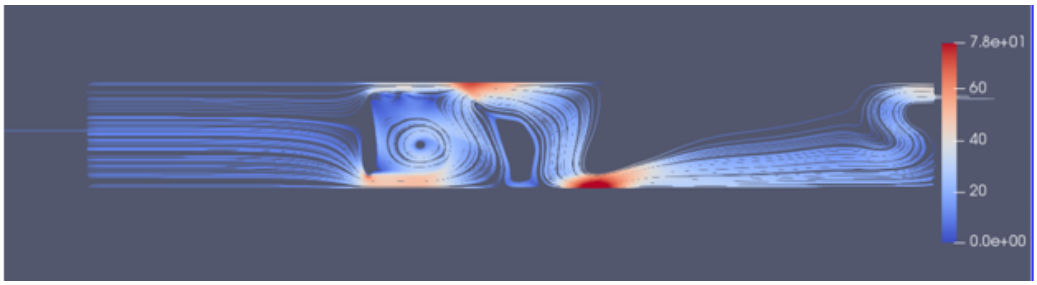

Figure 4-3: Streamlines at time = 52s

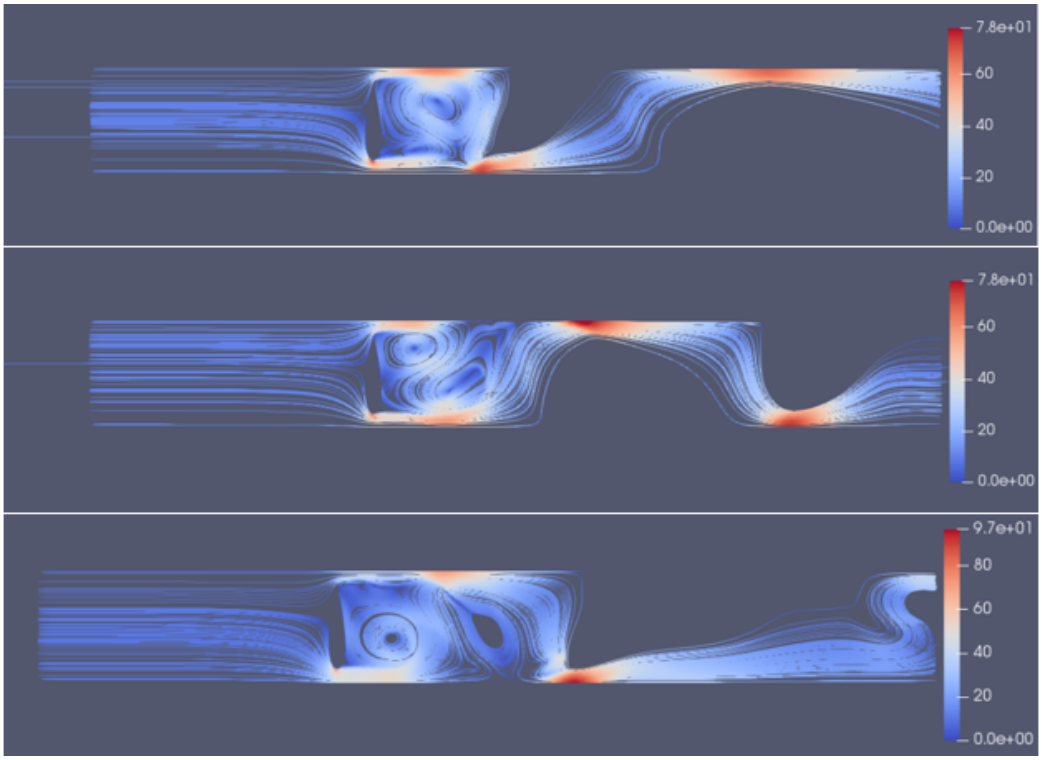

Figure 4-4: From top to bottom, Streamlines at times = 53s, 54s, and 55s

If we compare Figures 4-1, 4-2 and 4-3 to Figure 4-4, we can clearly state that this simulation is periodic and that the length of one period is equal to 3 seconds.

Another important thing to be noted from this comparison is that stable states can be considered at simulation times equal to 51s and 54s while the other two states of each period are transition states.

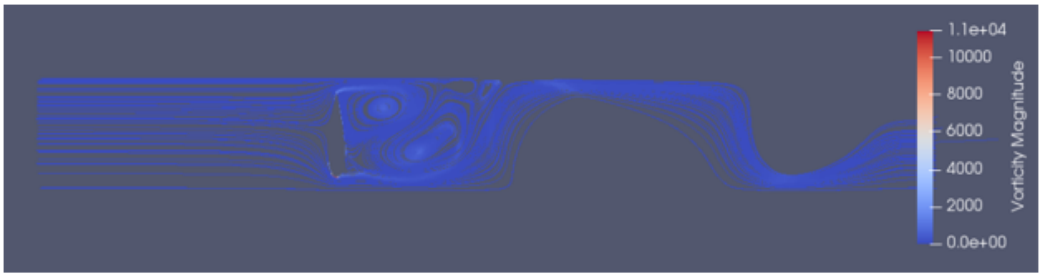

Figure 4-5: Vorticity Contours at time = 51s

One conclusion taken from Figure 4-5 can be that the reason for the 2 blank regions is that laminar flow is dominant there. If we zoom in around the tips of the airfoil, we can clearly see that the vorticity magnitude is higher at those two points than the rest of the domain, especially at the leading edge of the airfoil at the bottom.

Figure 4-6: Pressure Fields at time = 120s

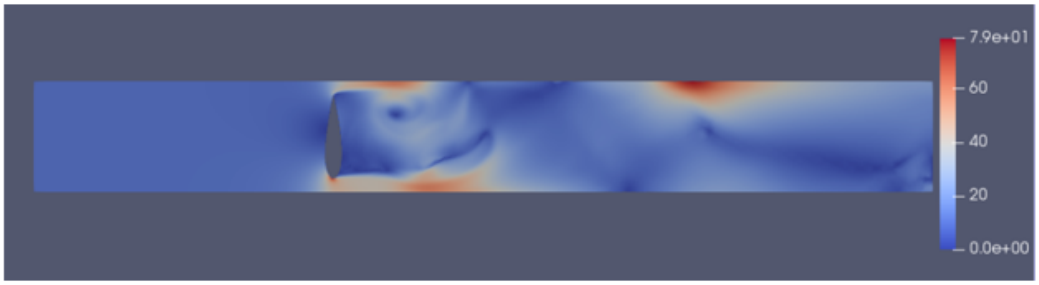

Figure 4-7: Velocity Fields at time = 120s

Von Karman vortices can be noticed in Figures 4-6 and 4-7, which means that we have a transient solution.

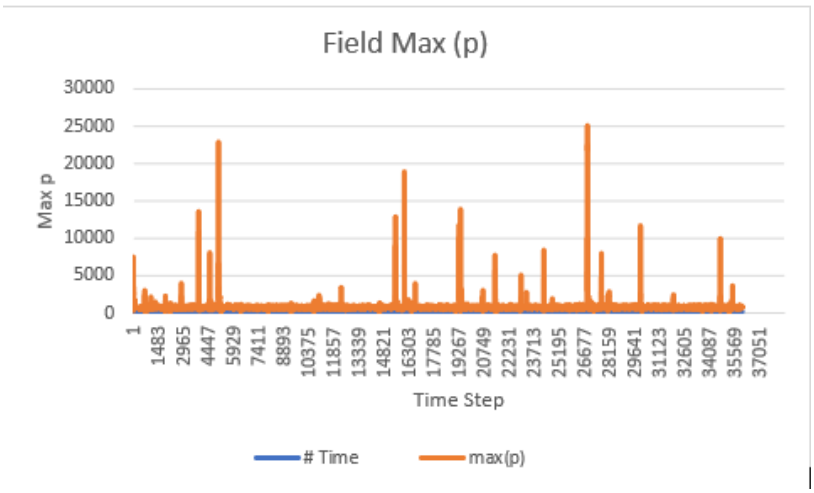

Figure 4-8: Max Field Pressure

As shown in Figure 4-8 the maximum field pressure was found to be 25100 Pascal at time = 134.255s, and the second tallest pike for the maximum pressure seen in the figure occurs at time = 25.164 and is equal to 22900 Pascal.

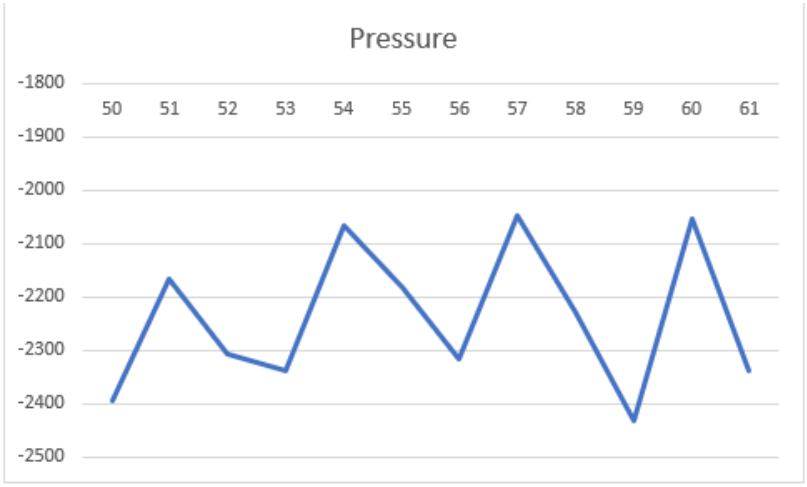

Figure 4-9: Pressure Probe at Leading Edge of the Airfoil

It can be seen from Figures 4-9 to 4-12 that the simulation is periodic and that one period is 3 seconds.

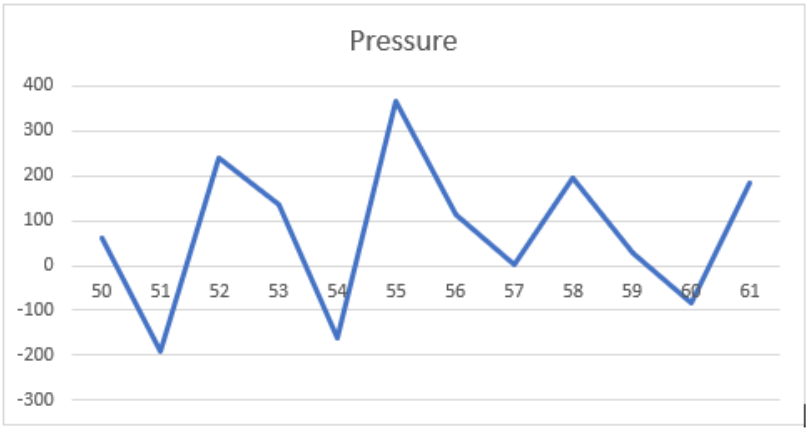

Figure 4-10: Pressure Probe at Trailing Edge of the Airfoil

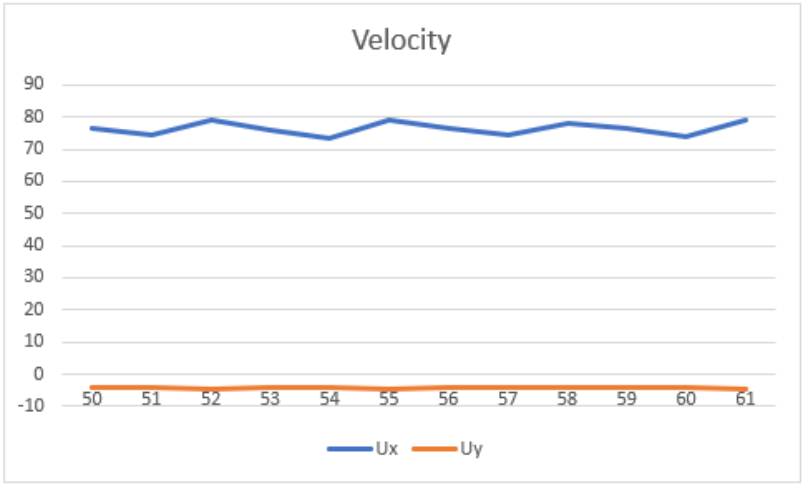

Figure 4-11: Velocity Probe at Leading Edge of the Airfoil

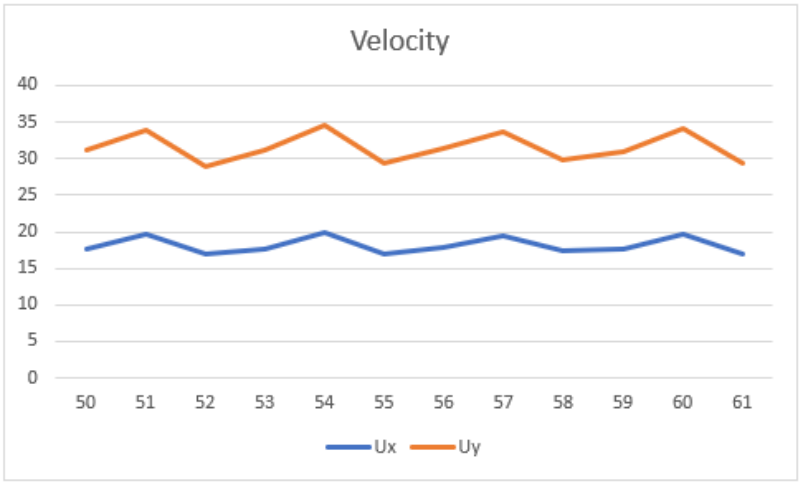

Figure 4-12: Velocity Probe at Trailing Edge of the Airfoil

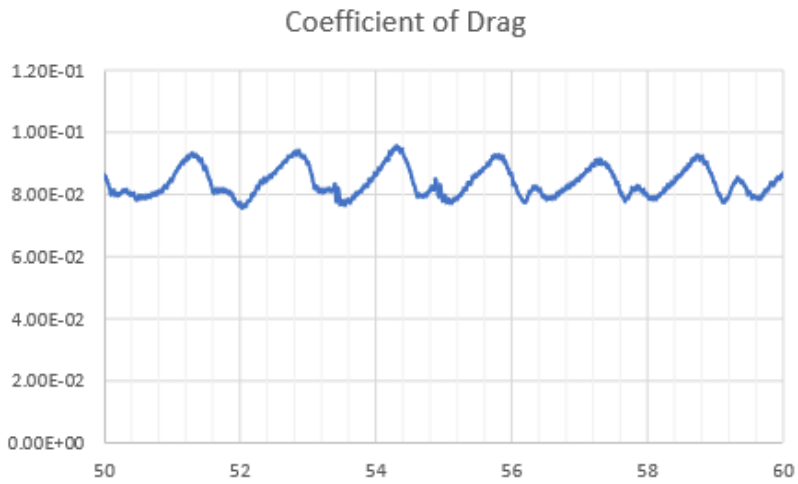

Figure 4-13: Drag coefficients at time =50 to 61s

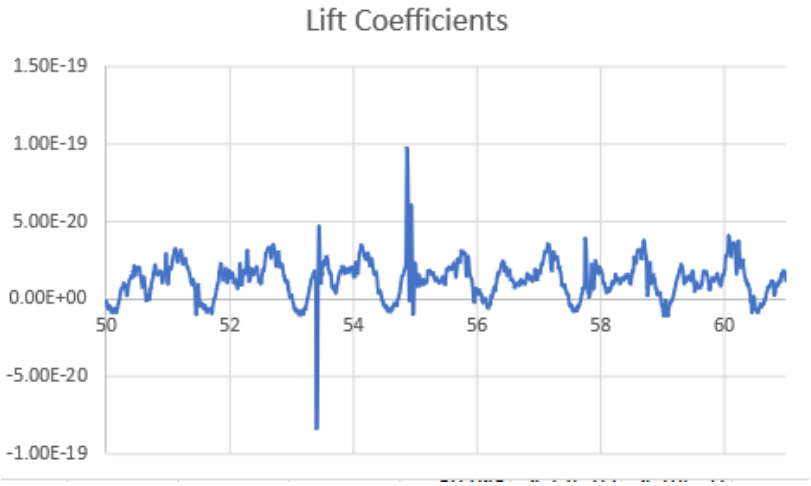

Figure 4-14: Lift coefficients at time =50 to 61s

4.2 Case 2: Sinusoidal Input

Figure4-15 shows the chosen oscillatory input airflow condition, which varies with time only in the axial direction. The equation for the axial velocity is $v_a = V_a.sin(2.\pi.t/T)$ where the amplitude Va is equal to 10m/s, and the period of the wave T is equal to 8 seconds. This means that the frequency is 0.125H.

As shown in table 4.2, the only change in boundary conditions from the constant input airflow condition case is for the Inlet. In this simulation case, which is an oscillatory input, the Inlet boundary condition is defined as a "uniformFixedValue" which

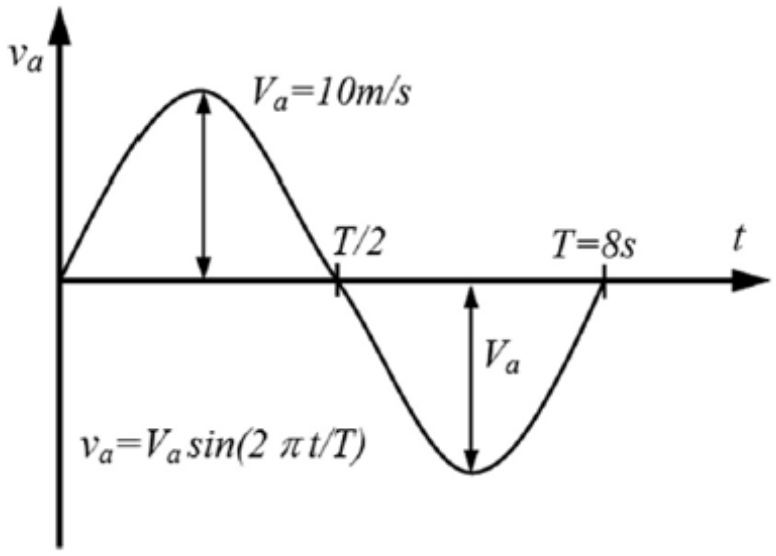

Figure 4-15: Axial Velocity Variation with Time

Table 4.2: Velocity Boundary Fields for Case 2

Boundary Field	**Type**
Inlet	uniformFixedValue
Outlet	inletOutlet
Top	slip
Bottom	slip
Back	empty
Front	empty
Airfoil	noSlip

extends the "fixedValue" boundary condition and allows the value to be prescribed as a function of time.

The simulation runs fine at first, but as the flow reverses at the inlet, an extremely high velocity occurs at the lower corner of the domain and the simulation crashes.

The second trial was carried out by using a "fixedMean" boundary condition. This boundary condition extrapolates field to the patch using the near-cell values and adjusts the distribution to match the specified, optionally time-varying, mean value. Even though it provides a more stable solution, it is not exactly what we are looking for, and so the solution will not be correct if this boundary condition was

used.

A third trial with two variations was conducted by using the same "uniformFixedValue" boundary condition as in the first trial, but this time a table was defined instead of sine. The oscillating input function was transformed into discrete values calculated over the whole period at equal time steps of 0.2. In the first trial of this method, both the positive and negative values of the input were taken into consideration. However, we faced the same problem that occurred earlier due to the negative values of the velocity in the second half of the period. In the second trial of this method, the negative values of the second part of the period were converted to positive values by taking the absolute value of all the velocities. We are faced with a stable solution, but still not a correct one.

After digging more into other possible solutions, it was learned that the "groovyBC" which can be found in Swak4Foam can be a feasible solution for this problem. Other boundary conditions worth trying are the "codedFixedValue" and "codedMixed" as they could also result in a good solution.

Chapter 5

Turbine-Chamber Coupling

5.1 Coupling Overview

As mentioned in earlier sections, the main elements of the OWC systems are the air turbine, and the chamber with the water column [41]. Many works focused on studying the performance of the OWC chamber, in parallel to other many works which centered around developing the OWC air turbines. However, most of these studies investigated the two main elements of the OWCs separately, for the sake of simplicity [42]. Accordingly, the air turbine and its effects on the pressure difference and oscillations of the water column in the chamber are neglected in the analysis of the chamber. Similarly, the oscillations of the water column and the pressure variations during the exhalation and inhalation processes are not considered in the analysis of the self-rectifying air turbines, whether Wells or impulse turbines [41].

In fact, one of the main factors that the overall performance of the OWC wave energy converter strongly depends on, is the coupling between the chamber and the air turbine as these two elements depend on each other. This coupling between the chamber and the turbine exerts a fundamental role in the design and optimization of the OWC converter [43], as it is in fact one of the critical aspects in the efficiency of these converters [44]. The turbine must provide the optimal pneumatic damping (pressure difference across the turbine) to achieve resonant or near-resonant conditions in the chamber. However, the difficulty lies in that this optimum damping depends

on the wave conditions. Moreover, the chamber must provide the optimal pneumatic energy to maximize the turbine production in turn [41, 42, 44].

The essential parameters to be considered and studied for the turbine-chamber coupling are: the pressure drop between the chamber and the atmosphere (Δp), the flow rate through the turbine duct per unit width of converter (q), and the characteristic dimension of the chamber, i.e. the chamber length (l) and the geometric characteristics of the OWC-chamber [42, 45]. Furthermore, the efficiency of the OWC chamber in transforming the wave power into pneumatic power is characterized by means of the capture factor [42, 44], which is defined as:

$$CF = \frac{P_p}{P_w} \tag{5.1}$$

Where P_p is the mean wave power of the incident waves per unit width of converter, and P_w is the mean pneumatic power per unit width of converter. However, the capture factor depends on the wave conditions and tidal level. Moreover, it depends on the damping that the turbine exerts on the system. Hence, to quantify this influence, a dimensionless damping coefficient is defined as [41, 42]:

$$B^* = \frac{\Delta p^{1/2}}{q} \frac{l}{\rho_a^{1/2}} \tag{5.2}$$

Where ρ_a is the air density, and l is the chamber length. The damping coefficient indicates, the ratio between the square root of the pressure drop and the flow rate for a given chamber geometry. Therefore, for a given wave condition, there will be a value of the damping coefficient that will maximize the capture factor of the OWC. In other words, an appropriate selection of damping coefficient increases the pneumatic power captured by the chamber substantially.

To get the maximum pneumatic power, the turbine damping must be close to the optimum chamber damping. The damping caused by a turbine relies mainly on its size, and on the rotation velocity [46]. Thus, when the optimum damping coefficient of the chamber is found, the turbine damping is determined and as a result the turbine diameter is estimated. Nevertheless, the chamber is working under a certain value

of the damping coefficient which is associated to a certain value of the pressure drop coefficient [42].

There are many factors that affect the capture factor such as: the damping induced by the turbine on the OWC chamber which is the ingredient that affects the capture factor the most, followed by the wave period, while the importance of the wave height is comparatively lower. The relevance of the damping induced by the turbine on the system to the chamber efficiency emphasizes the essential role of the turbine–chamber coupling: The turbine damping impacts the oscillations of the water column, which, in turn, give rise to the airflow that drives the turbine. Thus, selecting an appropriate turbine is a fundamental requirement for the chamber to perform well. Moreover, there is a value of the damping coefficient that maximizes the capture factor, which depends on the wave conditions. In general, the largest damping leads to the highest values of the capture factor across virtually all the wave conditions, expect the small periods and large wave heights. For a given value of the damping coefficient, the capture factor varies more dramatically when the wave period changes than when the wave height does. This means that the wave period is more relevant to the OWC performance than the wave height. Moreover, outside the range of the optimum damping, an over-damped chamber will perform better than an under-damped one. The tidal level also has an impact on the capture factor that depends on the damping value, as the capture factor increases with the tidal level with small and intermediate damping but decreases with the tidal level with large damping [42, 44].

5.2 Coupling Methods

One of the engineering problems that appears in a wide range of applications is the interaction between fluid and structure. This interaction is a phenomenon that occurs in nature as well, for example the the movement of sand dunes caused by wind. Solving such problems depends on the relations of continuum mechanics, and is mostly solved with numerical methods. However, the complex geometries, intricate physics of fluids, and complicated fluid-structure interactions make solving such prob-

lems a computational challenge. These processes can only be calculated using laws and equations from different physical fields, because the arising subproblems cannot be solved independently, such applications are called multiphysics applications. The fluid-structure interactions (FSIs) are an important class of these multiphysics problems. They are characterized by the fact that the flow around a body has a strong impact on the structure, and in turn; the modification of the structure has a considerable influence on the flow. The two fields involved in these kinds of multiphysics problems are fluid dynamics and structural dynamics, which can both be described by the relations of continuum mechanics [47].

Solution strategies for FSI simulations are mainly divided into monolithic and partitioned methods. Partitioned methods are divided into one-way and two-way coupling. Two-way coupling is further divided into weakly and strongly coupled methods. Regardless of whether one-way or two-way coupling methods are used, separate solutions for the different physical fields are prepared. One field that must be solved is fluid dynamics, the other is structure dynamics. The information for the solution is shared between the fluid solver and structure solver at the fluid-structure interface. This information is dependent on the coupling method. For example, only the fluid pressure acting at the structure is transferred to the structure solver in one-way coupling calculations, while the displacement of the structure is also transferred to the fluid solver in two-way-coupling calculations.

Generally speaking, for more accurate solutions, specifically for greater deflections where the fluid field is considerably affected by structural deformation, two-way-coupling surpasses one-way coupling. Furthermore, strong two-way coupling solutions can be of a second-order time accuracy and are more stable. The two-way method guarantees energy conservation at the interface, while the one-way does not. These are the main advantages of two-way coupling over one-way. On the other hand, the advantage of one-way coupling simulations is that it has a distinctly lower computational time. Moreover, the deformation of the fluid mesh does not need to be calculated in one-way coupling calculations, which provides a mesh of constant quality.

Chapter 6

Conclusion and Future Recommendations

6.1 Conclusion

This thesis work is a first step towards a long period project, the final aim of which is to reduce the noise generated by the turbine to spread the use of this type of superior renewable energy resource. The development of an acoustic model is a vital step towards reaching this goal and will be achieved through the collaboration of many researchers. However, the coupling of the turbine and the numerical wave tank, and thus, the modelling of the whole OWC system will be needed as a next step.

After surveying and reading a lot of technical literature, a representative turbine and air duct geometry were chosen to be followed and modelled. The geometry and mesh were created by the open-source pre-processing software GMSH. Simulation of different airflow conditions were carried out by using OpenFOAM, which proved to be a very useful tool for research purposes as the choices of a researcher are not limited or bounded there.

All in all, working with OpenFOAM requires a lot of time, dedication, and persistence as it is a huge and exciting adventure for anyone who wants to have a career in research. The learning curve is steep and the more experienced a person becomes,

the more there is to learn.

6.2 Future Recommendations

Future recommendations that can be implemented in the future work are listed as bellow:

- At one point, our numerical investigations will need to be validated by performing some experimental studies if possible, as they will prove useful for validating the results of coupling.
- The clearance between each tip of the airfoil and the adjacent wall should be increased to avoid adverse effects or problems with vortex shedding, and to improve turbine efficiency as well.
- A structured mesh can be used instead of an unstructured mesh, and the domain can be split into smaller regions that can be meshed separately. Improving and optimizing the mesh can greatly enhance the accuracy of the numerical simulations.
- The computational domain should be extended more in both directions, as a larger domain can ensure a higher development of flow. A much finer mesh should be used next to the top and bottom.
- A grid independency study should be made with three different grid sizes, a course, a medium and a fine mesh. The choice of cell numbers can be based on either previous experience or on literature.
- Cyclic boundary conditions should be defined at the Top and the Bottom patches, instead of walls, as the latter is wrong.
- A turbulence model should be used at the next stage, as the literature suggested using different turbulence models with various wall functions, and compare the results. Spallart Allmaras model or Realizable $k - \varepsilon$ turbulent model with

standard wall function can be good choices, as both can provide acceptable accuracy and time cost.

- For acoustic simulations, it is important to measure pressure fluctuations in principle, but more precisely the intensity in decibels (dB). Mach number can also be measured.

Bibliography

[1] M. Mamun. The study on the hysteretic characteristics of the wells turbine in a deep stall condition. 2006.

[2] Tom W Thorpe. An overview of wave energy technologies: status, performance, and costs. article. Technical report, 1999.

[3] H. Bouhrim and A. EL Marjani. On numerical modeling in owc systems for wave energy conversion. In *2014 International Renewable and Sustainable Energy Conference (IRSEC)*, pages 431–435, 2014.

[4] Tapas Kumar Das, Paresh Halder, and Abdus Samad. Optimal design of air turbines for oscillating water column wave energy systems: A review. *The International Journal of Ocean and Climate Systems*, 8(1):37–49, 2017.

[5] Antonio Falcao, João Henriques, and L.M.C Gato. Self-rectifying air turbines for wave energy conversion: A comparative analysis. *Renewable and Sustainable Energy Reviews*, 91, 04 2018.

[6] Ying Cui and Beom-Soo Hyun. Numerical study on wells turbine with penetrating blade tip treatments for wave energy conversion. *International Journal of Naval Architecture and Ocean Engineering*, 8, 07 2016.

[7] OpenFOAM. *OpenFOAM User Guide*, July 22, 2020. http://foam.sourceforge.net/docs/Guides-a4/OpenFOAMUserGuide-A4.pdf.

[8] Ying Cui, Zhen Liu, Xiaoxia Zhang, and Chuanli Xu. Review of cfd studies on axial-flow self-rectifying turbines for owc wave energy conversion. *Ocean Engineering*, 175:80–102, 02 2019.

[9] Antonio Falcao and João Henriques. Oscillating-water-column wave energy converters and air turbines: A review. *Renewable Energy*, 85:1391–1424, 01 2016.

[10] Jean-Roch Nader. Interaction of ocean waves with oscillating water column wave energy convertors. 2013.

[11] N. Delmonte, D. Barater, F. Giuliani, P. Cova, and G. Buticchi. Review of oscillating water column converters. *IEEE Transactions on Industry Applications*, 52(2):1698–1710, 2016.

[12] Gunnar Mørk, Steve Barstow, Alina Kabuth, and M. Pontes. Assessing the global wave energy potential. volume 3, 06 2010.

[13] Chongfei Sun, Jianzhong Shang, Zirong Luo, Zhongyue Lu, and Ruifang Wang. A review of wave energy extraction technology. *IOP Conference Series: Materials Science and Engineering*, 394:042038, 08 2018.

[14] António F. de O. Falcão. Wave energy utilization: A review of the technologies. *Renewable and Sustainable Energy Reviews*, 14(3):899 – 918, 2010.

[15] Iraide Lopez, Jon Andreu, Salvador Ceballos, Inigo Martinez de Alegria, and Iñigo Kortabarria. Review of wave energy technologies and the necessary power-equipment. *Renewable and Sustainable Energy Reviews*, 27:413–434, 11 2013.

[16] H. Titah-Benbouzid and M. Benbouzid. Ocean wave energy extraction: Up-to-date technologies review and evaluation. In *2014 International Power Electronics and Application Conference and Exposition*, pages 338–342, 2014.

[17] Irene Simonetti, Lorenzo Cappietti, Hisham Elsafti, and Hocine Oumeraci. Numerical modelling of fixed oscillating water column wave energy conversion devices: Toward geometry hydraulic optimization. 05 2015.

[18] V. Baudry, A. Babarit, and Alain Clément. An overview of analytical, numerical and experimental methods for modelling oscillating water columns. 09 2013.

[19] André Croft Moura, Márcia Carvalho, S. Patrício, Nuno Nunes, and C. Soares. Airborne and underwater noise assessment at the pico owc wave power plant. 2010.

[20] T. Setoguchi and M. Takao. Current status of self rectifying air turbines for wave energy conversion. *Energy Conversion and Management*, 47:2382–2396, 2006.

[21] Tom W Thorpe et al. *A brief review of wave energy*. Harwell Laboratory, Energy Technology Support Unit London, 1999.

[22] B Drew, A R Plummer, and M N Sahinkaya. A review of wave energy converter technology. *Proceedings of the Institution of Mechanical Engineers, Part A: Journal of Power and Energy*, 223(8):887–902, 2009.

[23] Johannes Falnes. A review of wave-energy extraction. *Marine Structures*, 20(4):185 – 201, 2007.

[24] Iraide López, Jon Andreu, Salvador Ceballos, Iñigo Martínez de Alegría, and Iñigo Kortabarria. Review of wave energy technologies and the necessary power-equipment. *Renewable and Sustainable Energy Reviews*, 27:413 – 434, 2013.

[25] Ahmed S. Shehata, Qing Xiao, Khalid M. Saqr, and Day Alexander. Wells turbine for wave energy conversion: a review. *International Journal of Energy Research*, 41(1):6–38, 2017.

[26] M. H. Mohamed. Design optimization of savonius and wells turbines. 2011.

[27] T Heath. A review of oscillating water columns. *Philosophical transactions. Series A, Mathematical, physical, and engineering sciences*, 370:235–45, 01 2012.

[28] J. Twidell. *Energy for Rural and Island Communities: Proceedings of the Conference, Held in Inverness, Scotland, 22-24 September 1980*. Pergamon Press, 1981.

[29] Zhen Liu, Chuanli Xu, Na Qu, Ying Cui, and Kilwon Kim. Overall performance evaluation of a model-scale owc wave energy converter. *Renewable Energy*, 149:1325 – 1338, 2020.

[30] Karthikeyan Thandayutham, A. Samad, A. Salam, D. Baruah, and Prasad Dudhgaonkar. Performance analysis of an air turbine for ocean energy extraction using cfd technique. *Journal of The Institution of Engineers (India): Series C*, 100:523–530, 2019.

[31] Mohammad Mamun. The study on the hysteretic characteristics of the wells turbine in a deep stall condition. *Energy and Material Science Graduate School of Science and Engineering*, 2004, 01 2006.

[32] I A Babintsev. Apparatus for converting sea wave energy into electrical energy. 12 1975.

[33] T Setoguchi, S Santhakumar, H Maeda, M Takao, and K Kaneko. A review of impulse turbines for wave energy conversion. *Renewable Energy*, 23(2):261 – 292, 2001.

[34] Stephen Stansfeld, Mary Haines, and Bea Brown. Noise and health in the urban environment. *Reviews on environmental health*, 15:43–82, 01 2000.

[35] Hans Slabbekoorn, Niels Bouton, Ilse Van Opzeeland, Aukje Coers, Carel Ten Cate, and Arthur Popper. A noisy spring: The impact of globally rising underwater sound levels on fish. *Trends in ecology & evolution*, 25:419–27, 07 2010.

[36] J. Hildebrand. Impacts of anthropogenic sound. 2005.

[37] S. Patrício, A. Moura, and T. Simas. Wave energy and underwater noise: State of art and uncertainties. *OCEANS 2009-EUROPE*, pages 1–5, 2009.

[38] Helen Bailey, Bridget Senior, Dave Simmons, Jan Rusin, Gordon Picken, and Paul Thompson. Assessing underwater noise levels during pile-driving at an offshore windfarm and its potential effects on marine mammals. *Marine pollution bulletin*, 60:888–97, 02 2010.

[39] FOSSEE. Openfoam: An open source alternative to commercial computational fluid dynamics (cfd) software. Brochure, 2018. https://static.fossee.in/cfd/brochures/Final_OpenFOAM_Brochure_2018.pdf.

[40] FOSSEE. Openfoam: Open source field operation and manipulation. Brochure, 2016. https://cfd.fossee.in/sites/default/files/brochures/CFD_OpenFoam_Brochure_3_2_2016.pdf.

[41] Ivan Lopez, Gregorio Iglesias, Mario López, Francisco Castro, and Miguel Rodríguez. Turbine–chamber coupling in an owc wave energy converter. volume 1, 10 2012.

[42] I. López, B. Pereiras, F. Castro, and G. Iglesias. Optimisation of turbine–induced damping for an owc wave energy converter using a rans–vof numerical model. *Applied Energy*, 127:105 – 114, 2014.

[43] R Curran, T P Stewart, and T J T Whittaker. Design synthesis of oscillating water column wave energy converters: Performance matching. *Proceedings of the Institution of Mechanical Engineers, Part A: Journal of Power and Energy*, 211(6):489–505, 1997.

[44] I. López, B. Pereiras, F. Castro, and G. Iglesias. Performance of owc wave energy converters: influence of turbine damping and tidal variability. *International Journal of Energy Research*, 39(4):472–483, 2015.

[45] H. Bouhrim and A. El Marjani. Turbine–chamber interactions analysis in an owc device for wave energy conversion. In *2015 3rd International Renewable and Sustainable Energy Conference (IRSEC)*, pages 1–6, 2015.

[46] F. Castro, M. Rodríguez, P. Valdez, I. Lopez, G. Iglesias, and B. Pereiras. An alternative approach to match the turbine to the characteristics of an owc wave power plant, Jan 2012. ISOPE.

[47] Friedrich-Karl Benra, Hans Josef Dohmen, Ji Pei, Sebastian Schuster, and Bo Wan. A comparison of one-way and two-way coupling methods for numerical analysis of fluid-structure interactions. *Journal of Applied Mathematics*, 2011:1–16, 2011.